CURRENT MICROBIOLOGY Vol. 25 (1992), pp. 319–325

Current Microbiology

Ultrastructure of *Nosema marucae* sp. n. (Microspora, Nosematidae), a Pathogen of *Maruca testulalis* (Lepidoptera, Pyralidae)

Maurice O. Odindo[1] and Walter G.Z.O. Jura[2]

[1]The International Center of Insect Physiology and Ecology (ICIPE), Mbita, Kenya; and [2]ICIPE, Nairobi, Kenya

Abstract. The development of *Nosema marucae* was followed in its host, the legume pod borer *Maruca testulalis*. The meronts had an irregular cell body and were binucleated, with the large diplokaryon occupying most of the cell. The sporonts contained many rough endoplastic reticula. The sporoblasts had a granular cytoplasm with a large number of ribosomes, and nuclear division and cellular cleavage were prevalent, particularly from 84 to 120 h after inoculation. Sporoblasts and young spores were evident from 108 to 144 h after inoculation.

In the mature spores, the exocuticle had a rough and sculptured surface and the endocuticle thinned considerably at the apical end. The anchoring disc was thick at the point of attachment. The polar tube had 12–15 loops, and the polaroplast was multilayered with two distinct regions and occupied almost half of the spore. The diplokaryon was centrally located in the cell; the nuclear membranes of the diplokarya were separated by an electron-dense region about 0.6 nm thick.

The legume pod borer *Maruca testulalis* is a major pest on legumes in Africa, South America, the Indian subcontinent, South and South East Asia, and parts of Australia [6]. Surveys for pathogens in the cowpea-growing areas of western Kenya showed that this pest is infected naturally by a *Nosema* sp. [16]. Several *Nosema* species have been described from pyralid hosts. *Nosema pyrausta* occurs in natural populations of the European corn borer *Ostrinia nubilalis* [1]. Records have been made of *N. manierae* infections in the rice pest *Chilo zacconius* [18]. Recent observations have also shown that *Nosema* species infect the poroporo stem borer *Sceliodes cordalis* [14].

In the present paper on fine structural studies on the microsporidian isolate from *M. testulalis*, the vegetative stages and spores of the pathogen are described.

Materials and Methods

Infection of borer larvae. *Maruca testulalis* larvae were reared on a natural diet, consisting of flowers and pods of the cowpea *Vigna unguiculata*, to the 3rd instar stage. Thirty larvae were starved overnight and inoculated with *Nosema* spores by feeding them on cowpea pods dipped into an aqueous suspension of the pathogen containing 1.5×10^6 spores/ml. The larvae were allowed to feed for 1 h; then they were placed on the fresh natural diet in sterilized petri dishes.

Preparation of specimens for histology. At 24 h after inoculation, and every 24 h subsequently, four larvae were removed from the diet and dissected in cold glutaraldehyde–cacodylate buffer (1 : 3) at pH 7.4. Portions of the fat body tissue, the hypodermis, and Malpighian tubules were incised off and fixed in fresh, cold, buffered glutaraldehyde, and processed further for electron microscopy according to the standard procedure for handling microsporidian spores [8]. Ultrathin sections were cut with glass knives on an LKB ultramicrotome, stained in uranyl acetate and lead citrate, and examined at 80 kV in a Philips 201 or CM 12 electron microscope.

Results

Structure of immature stages. The sporoplasm had an irregular cell body with a thin plasma membrane (Fig. 1). The cells were binucleated, with a large diplokaryon occupying most of the cell. The meronts

Address reprint requests to: Dr. M.O. Odindo, The International Centre of Insect Physiology and Ecology (ICIPE), P.O. Box 30, Mbita, S. Nyanza, Kenya.

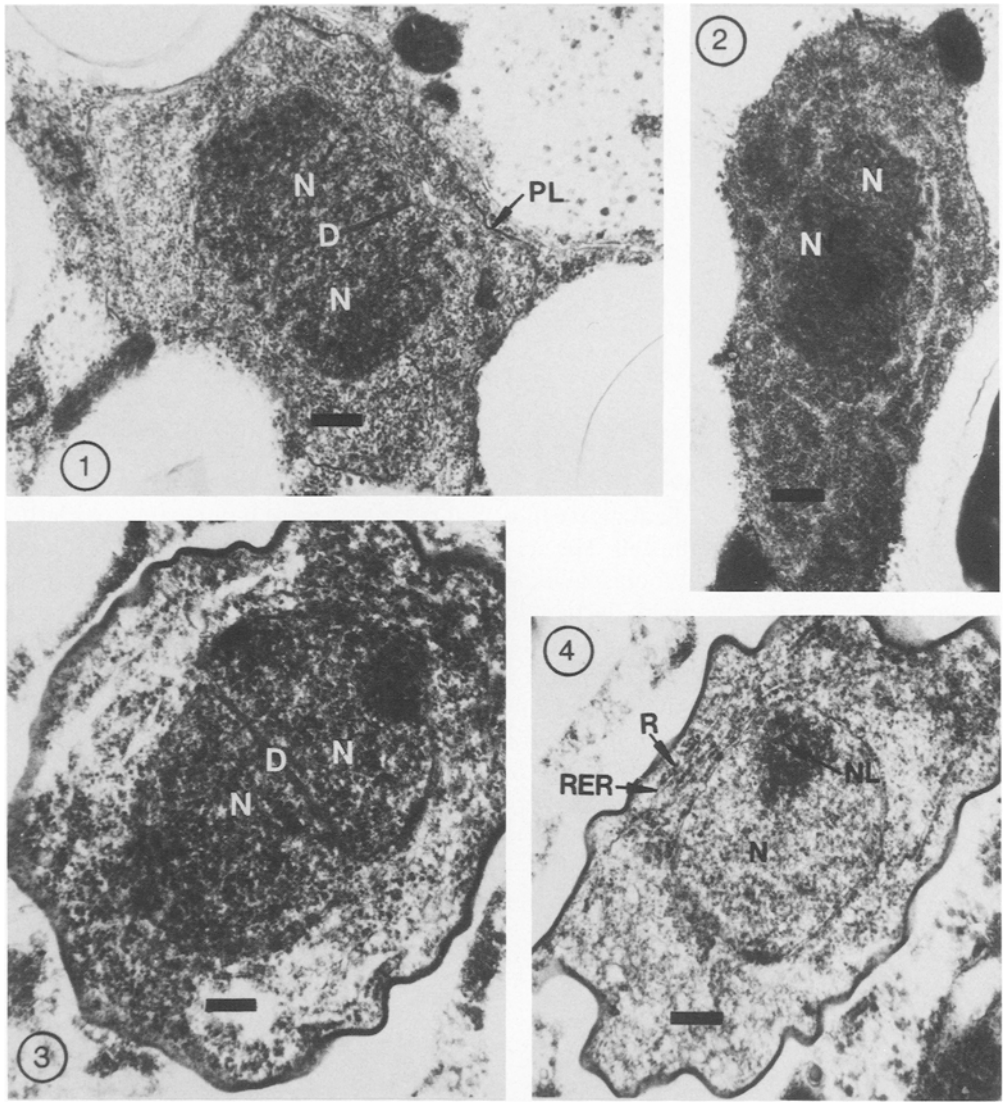

Figs. 1–4. Sporoplasm surrounded by plasm membrane (PL). The two nuclei (N) of the diplokaryon (D) occupy nearly half of the cell. Magnification, ×33,750; bar = 290 nm. Fig. 2. Young binucleated (N) meront. Magnification, × 26,000; bar = 390 nm. Fig. 3. Old meront. Magnification, × 49,000; bar = 200 nm. Fig. 4. Sporont with prominent nucleolus (NL) and profiles of rough endoplasmic reticulum (RER) and ribosomes (R). Magnification, × 42,000; bar = 240 nm.

(Figs. 2, 3) were also binucleated but had a well-defined plasma membrane. The sporonts were more elongate, had prominent nucleoli, and manifested well-developed profiles of the rough endoplasmic reticulum (Fig. 4). Tetranucleated sporonts (Fig. 5) were also commonly observed. Meronts and sporonts were abundant in tissues dissected from 84 to 120 h after inoculation. The sporoblasts were also binucleated and had well-defined nucleoli, as well as numerous ribosomes and rough endoplasmic reticulum in the cytoplasm (Figs. 6, 7). Initial development of the polaroplast and the anchoring disc was also manifested by the presence of their precursors within the cytoplasm of the sporoblast (Fig. 8).

During maturation, the spores became regular in shape, and the spore wall increased in thickness. The organelles of the spore became differentiated and distinctive. In the young spores the cross-section of the polar tube was clearly defined (Fig. 9), although it was not regularly arranged in the periphery of the sporoplasm as occurs in the mature spores. The primordia of the polaroplast, the anchor-

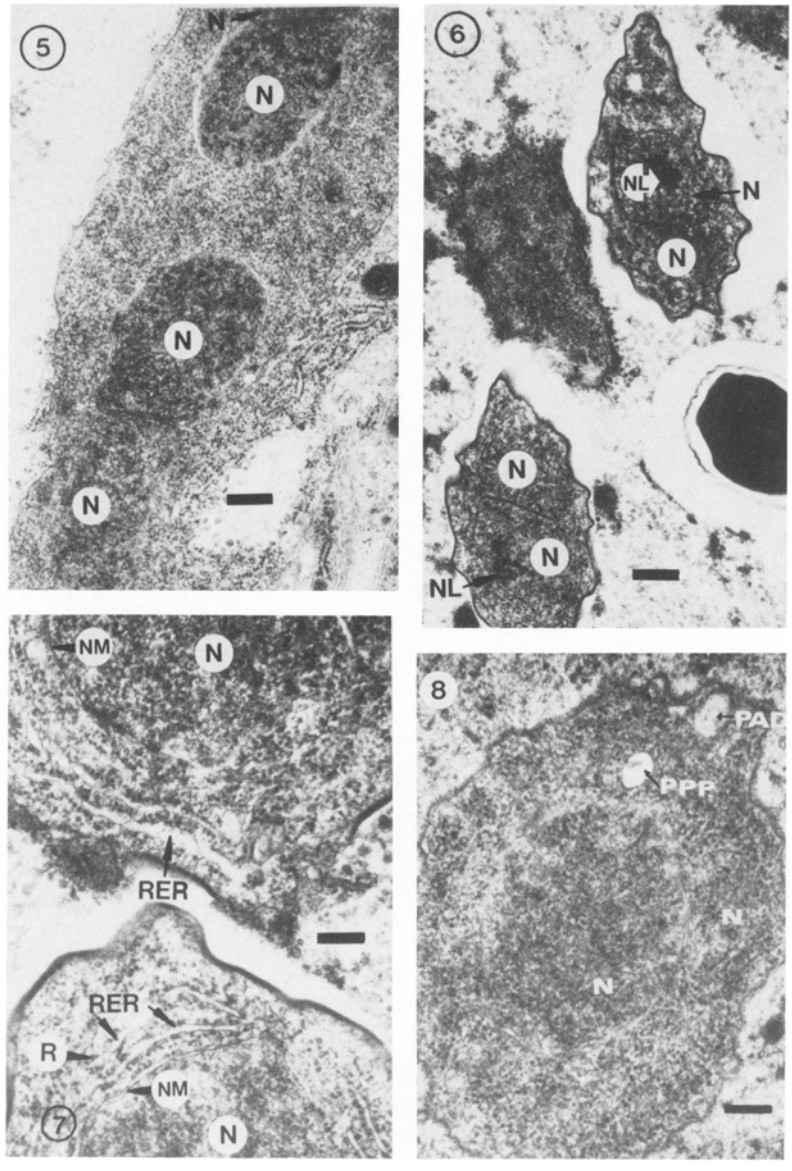

Figs. 5–8. Tetranucleated (N) sporont. Magnification, ×34,000; bar = 290 nm. Fig. 6. Sporoblasts with large nuclei (N) and prominent nucleoli (NL). Magnification, ×26,000; bar = 390 nm. Fig. 7. A section of the sporoblast showing ribosomes (R), rough endoplasmic reticulum (RER), and the nucleus surrounded by the nuclear membrane (NM). Magnification, × 52,500; bar = 190 nm. Fig. 8. Sporoblast showing the precursors of the anchoring disc (PAD) and the polaroplast (PPP). Magnification, × 52,500; bar = 190 nm.

ing disc, and the root of the polar tube were noticeable at the anterior region of the cell (Fig. 9). Sporoblasts and young spores were numerous from 108 to 144 h after inoculation.

Description of mature spores. The mature spores were ovoid, measuring 2.71 × 1.93 μm to 6.45 × 2.71 μm, and had a well-defined spore wall. On the exterior aspect, the spore wall was sculptured into irregular contours (Fig. 10). The thickness of the electron-dense exospore ranged from 22 to 66 nm, while the electron-luscent endospores was 50 to 69 nm thick and narrowed at the anterior end of the spore to a layer 4 nm thick near the anchoring disc (Figs. 10–12). The polar tube consisted of 12–15 rings (Figs. 10, 12). A cross-section through the polar tube showed that it was composed of three or four membranes and an electron-dense core (Fig. 12). The coils of the polar tube were arranged in a regular order at the periphery of the cytoplasm, 12–44 nm below the plasmalemma. The diameter of the coils was uniform throughout and measured, on average, 57 nm. The coils were arranged in such a way that the first were 12.5 nm apart and the rest were contiguous. The plasmalemma appeared as a thin membrane, 1.9 nm thick.

The polar tube was connected to the anterior tip of the spore on an umbrella-shaped anchoring disc

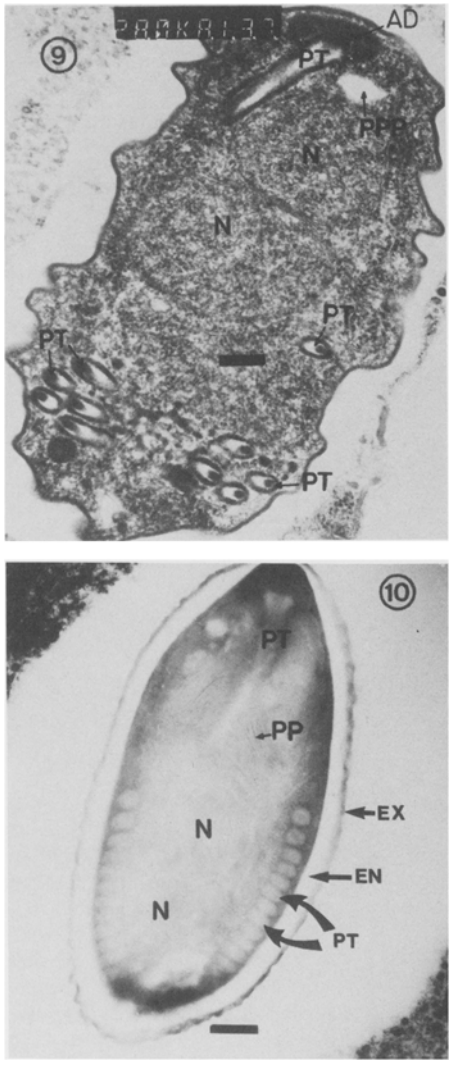

Figs. 9 and 10. Young spore showing the anchoring disc (AD), the polar tube (PT), and the precursor of the polaroplast (PPP). Posteriorly, the polar tubes (PT) are clearly seen, though they are not yet arranged at the periphery of the cell. Magnification, ×42,000; bar = 240 nm. Fig. 10. Mature spore showing the polaroplast (PP), polar tube (PT), and a prominent spore wall composed of the exospore (EX) and endospore (EN). Magnification, ×45,000; bar = 220 nm.

(Fig. 11). At its root on the anchoring disc, the tube was rounded and seemed to fit into a socket in the disc (Fig. 11). The polar tube was straight for the first one-fifth of the length of the spore, then coiled into 12–15 loops, 12–44 nm beneath the plasmalemma, with an angle of tilt of 83°.

The polaroplast consisted of two types of membranes, or lamellae. Anteriorly, and extending about one-third of the length of the spore, it consisted of thin, tightly packed lamellae in 12–30 layers (Fig. 11), each about 2.2 nm thick. Below these were larger and loosely packed lamellae of irregular shape, each measuring 9.9 nm thick (Fig. 11). The polaroplast occupied nearly half of the entire length of the mature spore, from the anchoring disc to the diplokaryon (Figs. 10, 11). The binucleated diplokaryon occupied the area surrounded by the coils of the polar tube and was located centrally in the cytoplasm. The nuclear membranes of the diplokaryon did not touch and were separated by an electron-dense region about 0.6 nm thick.

In insects infected for periods in excess of 160 h, the tissues bore numerous mature spores (Fig. 13). There was a high localization of infection in some cells, including spherical hemocytes and such tissues such as the fat body and Malpighian tubules. Second-generation meronts were noted among the mature spores (Fig. 13).

Spores which had discharged the sporoplasm were frequently observed (Fig. 14), particularly in tissue fixed at 160 h after inoculation.

Discussion

The structure of the developmental stages of *Nosema marucae* follows a pattern consistent with the genus *Nosema*, as described in other lepidopteran hosts [2, 14, 15, 18]. The basic morphology of the mature spores is also similar to other *Nosema* species.

In the vegetative stages, the binucleate meronts and sporonts were numerous, particularly in larvae dissected 84 h after infection. This is a period when there is fast multiplication of the pathogen, and larval mortality starts around this time. In earlier unpublished observations, we had observed some tetranucleated meronts as well as the binucleated ones. We also noted that some sporonts undergo a cyclic development in which the cellular division occurring at sporogony at 60–84 h does not lead to formation of sporoblasts, but instead results in a large number of sporonts.

The basic morphology of mature spores of *N. marucae* is also similar to other *Nosema* species, including the binucleate diplokaryon, and lamellate polaroplast [9]. The spore wall was observed to be rough and sculptured, as seen from the outline of spores cut in cross-section. Other forms of spore surface have been recorded in various *Nosema* species, including smooth in *N. lymantriae*; wrinkled in *N. bombycis*, *N. heliothidis*, *N. ploidae*, *N. tortricis* [11]; smooth in *N. blissi* [10]; and rough in *N. whitei* [7]. The surface of *N. tractabile*, a pathogen of the

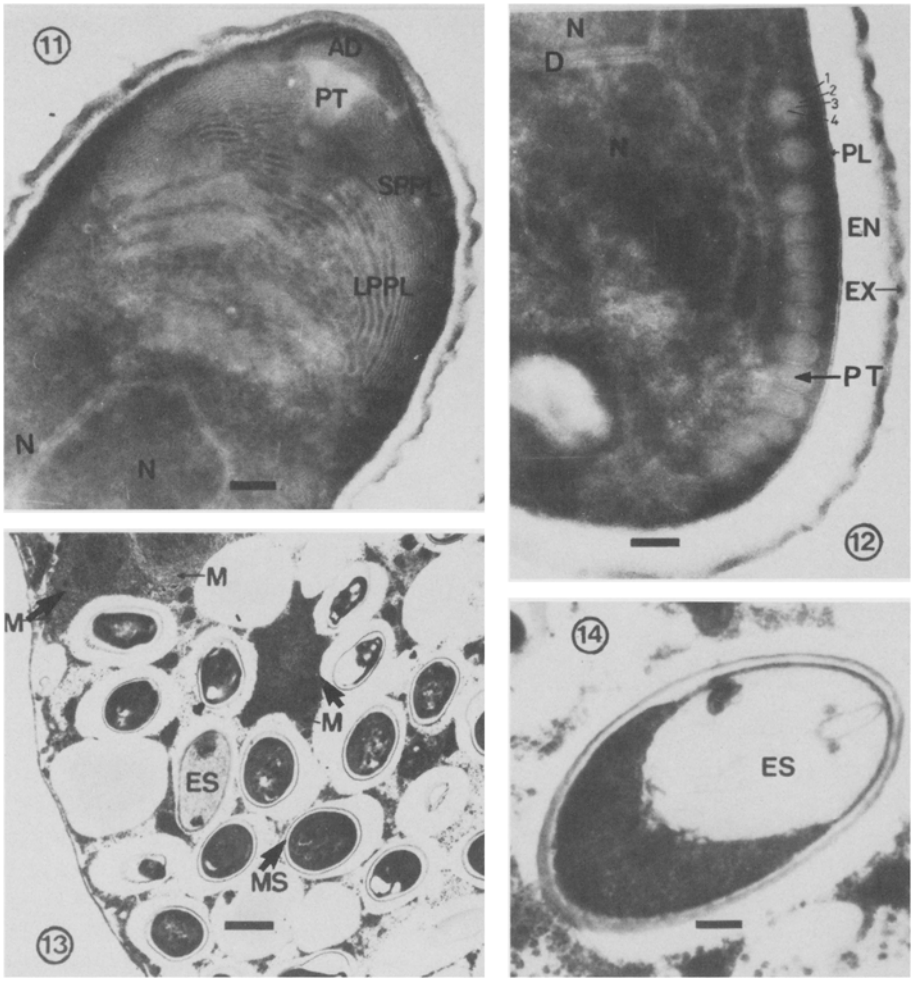

Figs. 11–14. Micrograph of the anterior part of a mature spore showing the two parts of the polaroplast, the small polaroplast lamellae (SPPL), and large polaroplast lamellae (LPPL). The umbrella-like anchoring disc (AD), polar tube (PT), and nucleus (N) are also shown. Magnification, ×90,000; bar = 110 nm. Fig. 12. A section of the posterior portion of a mature spore showing the two nuclei (N) of the diplokaryon (D), the plasmalemma (PL), the coils of the polar tube (PT), and the two parts of the sporewall, the endospore (EN) and exospore (EX). The numbers 1–4 refer to the membranes of the polar tube. Magnification, ×162,000; bar = 60 nm. Fig. 13. Section through the fat body showing mature spores (MS), extruded spores (ES), and the second-generation meronts (M). Magnification, ×7000; bar = 1.42 μm. Fig. 14. Mature spore with the sporoplasm already discharged (ES). Magnification, ×30,000; bar = 330 nm.

freshwater leech *Helobdella stagnalis*, was slightly rough and without sculpturing [8].

The polar tube is an important diagnostic character among the microsporidia. The number of polar tube coils, and the angle of tilt of the anterior coil were shown to be different in the various species that were studied [3], and the angle of tilt varied from 31° in *N. oryzaephili* to 86° in *N. spelotremae* [3]. In *N. tractabile*, it was observed that the angle of tilt of the polar tube was 55° [8]. In the present observations in *N. marucae*, the angle of tilt was 83°, in extremely tight coils.

The polar tube shows variation in dimensions, fine structure, regional specializations, and the number and arrangement of coils, all of which are important diagnostic tools for microsporidia [8]. For example, the length of the polar tubes in spores of a *Nosema* sp. in *Sceliodes cordalis* was recorded as 79, 82, and 107 μm [13], while in *N. tractabile*, an extruded tube was recorded as about 90 μm long [8]. In *N. herpobdellae*, polar tubes up to 150 μm long were observed [5], though they were usually 100–120 μm long. The number of coils of the tube has also been shown to vary from 12 in *N. eurytremae* [4] to 13–14 in *N. tractabile* [8]. In *N. marucae*, 12–15 coils were recorded. The details of the fine structure

Table 1. Properties of spores from some *Nosema* species

Species	Host	Infected tissues	Spore size (μm)	Polar tube		Reference
				Number of coils	Angle of tilt	
Nosema bombycis	*Chilo simplex*	Gut epithellal cells	3.0–4.0 × 1.5–2.0	-[a]	-[a]	[17]
Nosema eurytremae	*Trematodes*	—		12	41°	[4]
Nosema gasti	*Heliothis zea*	Gut epithelial cells	4.16–2.29	—	—	[13]
Nosema heliothidis	*Heliothis virescens*	Many tissues	2.5–5.5 × 1.7–2.2	—	—	[12]
Nosema herpobdellae	*Herpobdella octoculata* of digestive tract	Connective tissue	6.0–10.0 × 3.0–4.0	—	—	[5]
Nosema manierae	*Chilo zacconius*	Fat body, midgut, muscle, hypodermis, Malpighian tubules, salivary glands	3.7–4.4 × 2.2–2.6	—	—	[18]
Nosema sphingidis	*Manduca sexta*	Midgut, many tissues	4.3 × 2.2	—	—	[2]
Nosema tractabile	*Helobdella stagnalis*	Coelomocytes, ovaries, mesenchyme, epidermal glands, testes	3.5–4.0 × 2.1–2.5	13–14	55°	[8]
Nosema trichoplusiae	*Heliothis zea*	Gut epithelial cells	3.0–4.0 × 1.9–2.1	—	—	[15]
Nosema sp.	*Sceliodes cordalis*	Fat body, gut, Malpighian tubules	3.7–4.5 × 2.1–2.4	—	—	[14]

[a] Not specified

of the polar tube have not been recorded in most *Nosema* species, but in *N. tractabile* it was noted that the polar tube was made up of a large number of membranes, possibly up to 21 [8]. The rather large polaroplast may also be a significant feature of *N. marucae*. The polaroplast occupied close to 45% of the cell.

Other characteristics of significance in *Nosema* spp. are the shape of the spores and spore measurements. In *N. marucae* the spores were basically oval in shape and ranged in size from 2.7 to 6.5 μm × 1.9–2.7 μm. Both of these characteristics fall within the description of other *Nosema* spp. The general range of spore sizes observed in some *Nosema* species is given in Table 1 and indicates that, with the exception of *N. herpobdellae*, a parasite of *Herpobdella octoculata* in which spore measurements of up to 10 μm × 3.5–4 μm have been recorded [5]; most spore sizes range from 3–5 μm × 2–3 μm.

Description

Nosema marucae

Host: Legume pod borer *Maruca testulalis*, larvae, pupae, and adult.

Merogony: Meronts of three types: small binucleate; large binucleate; large tetranucleate.

Sporogony: Sporonts of two types: small binucleate; large binucleate.

Spore: Ovoid, 2.71 × 1.93 μm to 6.45 × 2.71 μm in fixed smears. The exospore is 22–66 nm thick, and the endospore, 50–69 nm; the plasmalemma is 1.9 nm thick. The polar tube has 12–15 rings and in cross-section has 3–4 layers; the diameter of the polar tube is 57 nm. The polaroplast consists of thin, tightly packed lamellae anteriorly and large loose lamellae posteriorly. The spore is binucleated, and the diplokaryon occupies a central area of the endosplasm surrounded by the coiled polar tube.

Tissues infected: Fat body, Malpighian tubules, integumental epithelial cells, tracheal epithelial cells, heart, inter-membrane tissue, and hemocytes.

Transmission: Horizontal transmission is prevalent, mostly through spores released from broken-down larval cadavers. Vertical transmission is also common and appears to be the usual mode of transmission of the pathogen in the field.

ACKNOWLEDGMENTS

We are grateful to Mr. Mathayo M.B. Chimtawi and Mrs. J. Muriithi for their excellent technical assistance during these studies. We are also grateful to Mr. P. Lisamula and Mr. W. Kiluva for the preparation of illustrations, and to Dr. A.N. Mengech for a critical review of the manuscript. This work was supported by a grant from International Fund for Agricultural Development (IFAD).

Literature Cited

1. Andreadis TG (1986) Dissemination of *Nosema pyrausta* in feral populations of the European corn borer, *Ostrinia nubilalis*. J Invertebr Pathol 84:335–343
2. Brooks WM (1970) *Nosema sphingidis* sp. n., a microsporidian parasite of the tobacco hornworm, *Manduca sexta*. J Invertebr Pathol 166:390–399
3. Burges HD, Canning EU, Hull IK (1974) Ultrastructure of *Nosema oryzaephili* and the taxonomic value of the polar filament. J Invertebr Pathol 23:135–139
4. Colley FC, Joe K, Zaman V, Canning EU (1975) Light and electron microscopical study of *Nosema eurytremae*. J Invertebr Pathol 26:11–205
5. Conet ME (1931) *Nosema herpobdellae*, Microsporidiae nouvelle parasite de Hirudinees. Ann Soc Sci Bruxelles 51:170–171
6. COPR (1981) Pest control in tropical grain legumes. London: Centre for Overseas Pest Research
7. Fowler JL, Reeves E (1975) Microsporidian spore structure as revealed by scanning electron microscopy. J Invertebr Pathol 26:1–6
8. Larsson R (1981) Description of *Nosema tractabile* n. sp. (Microspora, Nosematidae), a parasite of the leech *Heldobdella stagnalis* (L) (Hirudinea, Glossiphiniidae). Protistologica 17:407–422
9. Larsson R (1988) Identification of microsporidian genera (Protozoa, Microspora)—a guide with comments of the taxonomy. Arch Protistenkd 136:1–37
10. Liu HJ, McEwen L (177) *Nosema blissi* sp. n. (Microsporda: Nosematidae), a pathogen of the chinch bug *Blissus leucopterus hirtus* (Hemiptera: Lygaeidae). J Invertebr Pathol 29:141–146
11. Lom J, Weiser J (1972) Surface pattern of some microsporidian spores as seen in the scanning electron microscope. Folia Parasitol (Praha) 19:350–363
12. Lutz A, Splendore A (1904) Über Pebrine und verwandte Mikrosporidien. Nachtrag zur ersten Mitteilung. Zentrabl Bacteriol I Orig 46:645–650
13. McLaughlin RE (1969) *Glugea gasti* sp. n. microsporidian pathogen of the boll weevil, *Anthonomus grandis*. J Invertebr Pathol 16:84–88
14. Mercer CF, Wigley PJ (1987) A microsporidian pathogen of the poroporo stem borer *Sceliodes cordalis* (Dbld) (Lepidoptera, Pyralidae) I. Description and identification. J Invertebr Pathol 49:93–101
15. Nordin GL, Maddox JV (1974) Microsporida of the fall webworm, *Hyphantria cunea*. I. Identification, distribution, and comparison of *Nosema* sp. with similar *Nosema* sp. from other Lepidoptera. J Invertebr Pathol 24:1–13
16. Odindo MO, Otieno WA, Oloo GW, Kilori JT, Odhiambo RC (1989) Prevalence of microorganisms in field-sampled borers on sorghum maize and cowpea in western Kenya. Insect Sci Applic 10:225–228
17. Oshima K (1937) On the function of the polar filament of *Nosema bombycis*. Parasitology 29:220–224
18. Toguebaye B-S, Bouix G (1983) *Nosema manierae* sp.n., microsporidie parasite de *Chilo zacconius* Blezenski 1970 (Lepidoptera: Pyralidae), hôte naturel, et *Heliothis amigera* (Hubner 1808) (Lepidoptera: Noctuidae), hôte experimental: cycle evolutif et ultrastructure. Z Parasitenkd 69:191–205